AQUA
Water Infrastructure, Ecosystems and Society

 AQUA — Water Infrastructure, Ecosystems and Society Vol 72 No 7, 1344 doi: 10.2166/aqua.2023.108

On the effect of green nonstructural materials on scour reduction downstream of grid dissipators

Rasoul Daneshfaraz[a,*], Mehdi Rezaie[a], Ehsan Aminvash[a], Veli Süme[b], John Abraham[c] and Amir Ghaderi[d]

[a] Department of Civil Engineering, Faculty of Engineering, University of Maragheh, Maragheh, Iran
[b] Department of Hydraulics, Civil Engineering, Faculty of Engineering and Architecture, Recep Tayyip Erdoğan University, Rize, Türkiye
[c] School of Engineering, University of St. Thomas, St. Paul, USA
[d] Department of Engineering, Urmia University, Urmia 57561-15311, Iran
*Corresponding author. E-mail: daneshfaraz@yahoo.com

RD, 0000-0003-1012-8342; EA, 0000-0001-8901-2232; VS, 0000-0001-8251-2461; JA, 0000-0002-3818-8681; AG, 0000-0002-8661-6302

ABSTRACT

In this study, a nonstructural and eco-friendly solution has been used to reduce scouring downstream of screens. Upstream of the screen are stilling basins protected against scouring, but downstream locations are subjected to flow scouring. One of the challenges that the current research brings with it is the process of dispersing nanomaterials. In this research, to achieve its goals, three beds of channels with sedimentary materials, sedimentary materials plus clay, as well as sedimentary materials with a combination of clay and montmorillonite nanoclay have been used. The experimental results show the positive effect of clay and nanoclay on scour depth reduction downstream of the screens. The best performance occurs with the clay and montmorillonite clay mixture. The positive effect of clay and montmorillonite nanoclay mixture for scour length reduction is observed, and by utilizing this mixture, the length of scouring has decreased 33%. Furthermore, by adding clay and montmorillonite nanoclay mixture, the scour depth is reduced up to 39 and 46%, respectively. Utilizing clay and montmorillonite nanoclay mixture has a positive effect on scouring control. It could be very useful for cases such as rivers where bed protection with concrete is not possible.

Key words: downstream scouring, montmorillonite nanoclay, nanoclay, screens

HIGHLIGHTS

- Using nonstructural materials to control downstream scouring.
- Using new environmentally friendly materials to control downstream scouring.
- Using the combination of clay and montmorillonite nanoclay to control scouring and stabilize the bed for the first time.

GRAPHICAL ABSTRACT

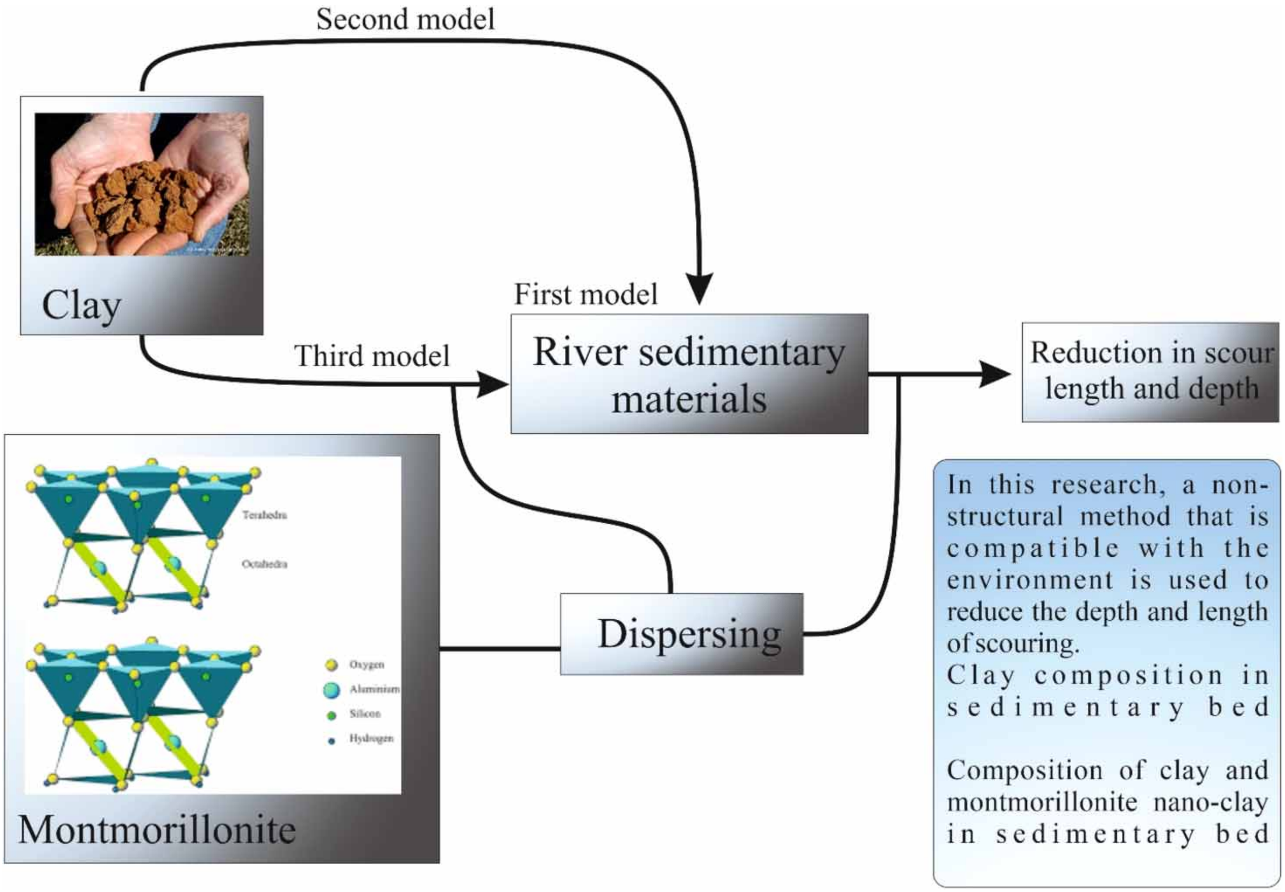

1. INTRODUCTION

Experimental research shows that screens positioned perpendicular to a supercritical flow path can dissipate flow energy (Rajaratnam & Hurtig 2000; Bozkus *et al.* 2007; Sadeghfam *et al.* 2014). Supercritical flow is created through a sluice gate; energy dissipation and hydraulic jump occur in the gap between the gate and the screen, which is called the stilling basin. After leaving the stilling basin, the flow will enter an unprotected area; one aim of this study is to reduce the length and depth of the scour hole in this area. The importance of scour investigation is revealed when the scour depth is significant. This is so that this scour reaches the foundation of river structures or moves or endangers the stability of these structures. On the other hand, construction materials such as concrete used to stabilize the bed can also have harmful environmental effects. One of the challenges that the current research brings with it is the process of dispersing nanomaterials. Due to the use of nano in the sedimentary bed, we cannot use it directly in the bed. For this purpose, we have to use dispersing materials to separate nanoparticles. The challenge that arises here is that the process of dispersing nanomaterials is a long and time-consuming process that requires high precision. But the advantage that this challenge brings is the drastic reduction of the scouring phenomenon. However, the advantages of using nanomaterials are more than the difficulties and time. Among other challenges, we can point out that nanomaterials should not be allowed to agglomerate after dispersing. Because in this case, the obtained results will not bring a positive result. On the other hand, these nanomaterials are environmentally-friendly and do not harm the environment.

Several studies in the field of downstream scouring of hydraulic structures have been conducted by researchers such as Chabert & Engeldinger (1956), Lee *et al.* (1961), Chiew (1992), Zarrati *et al.* (2004), Sanoussi & Habib (2008), Karimaee & Zarrati (2011), Singh & Maiti (2012), Elsebaie (2013), and Nasr-Allah *et al.* (2016). Tuna & Amiroglu (2011, 2013), Abdelhaleem (2003), and Elnikhely (2016) studied the downstream scouring of stepped and other spillways. They also investigated the effect of water depth and hydraulic conditions of the flow on the downstream scouring rate. Goel (2010) investigated scouring around bridge piers and geometrical changes in scouring (length, depth, and volume). The results indicated an increase in scouring geometrical parameters with an increasing flow rate. Lu *et al.* (2021) evaluated the hydrochemical evolution of pore water in the sedimentary zone of the riverbed during the infiltration of its bank. The results of their research showed that in the process of infiltration of river water, a series of redox reactions occur in the sedimentation area of the bed, and there are differences in different infiltration depths where strong respiration and denitrification occur.

Sun *et al.* (2021) used the combined model of support vector regression and the fruit fly optimization algorithm to predict scouring caused by ski-jump and reached the conclusion that the proposed method of support vector regression significantly improved the results of the support vector machine. Li *et al.* (2021) investigated sediment avoidance diversion and the coordinated dispatch of water and sediment at an injection-water supply project on a sediment-laden river. The results showed that during a period with high sediment content, large-scale silting occurs in a diversion channel. Also, to reduce sediment in a diversion channel, strategies have been presented to reduce mud. Jia *et al.* (2022) numerically evaluated the effect of obstruction on eddy flow in partly obstructed channels and showed that two vortex evolution patterns including sequent sole along-canopy vortices (SCVs) and alternating hybrid along-canopy and along-wall paired vortices (HCWVs) correspond to small and large blocking ratios, respectively.

Widyastuti *et al.* (2022) investigated the energy of dam failure with a porous structure in order to cope with scouring around bridge foundations. The results of laboratory studies showed that the percentage of friction speed in the energy containment area before and after the porous structures decreased by 31.42% and increased by 9.27%, respectively. Qasim *et al.* (2022) investigated the effect of channel bed roughness on the hydraulic parameters of a weir gate. The research showed that there are certain results between the Reynolds number and the downstream Froude number, the flow rate and the flow velocity in the downstream of the flow area passing through the gate and the downstream Froude number.

The methods that researchers have used to prevent scouring are placing structures in and near the place of scouring or changing the destructive flow pattern. The proposed method of this research is a new one that can be used along with other methods that will not disturb the river environment. In this research, a suitable solution to reduce the aforementioned problems by using materials compatible with the nature and ecology of the river and with the aim of reducing the downstream scouring depth of the hydraulic structures is provided. On the other hand, the length and depth of downstream scouring of recently used screens have not been fully evaluated so far, and the necessity of studying it has been felt by the authors of this study.

The research that has been done in the previous studies is related to the structural methods to reduce the amount of scour in the mobile bed or around the bridge piers. Meanwhile, in the present study, an attempt has been made to reduce the scouring rate of the mobile bed by using nonstructural and environmentally friendly methods. For this reason, in this research, the effect of adding clay and the combination of clay and montmorillonite nanoclay to sedimentary materials downstream of screens has been investigated in order to reduce the depth and length of scouring. To import clay or a mixture of clay and montmorillonite nanoclay, the grouting method is used at the maximum depth equivalent to the scouring of the no-clay layer or a mixture of clay and nanoclay.

2. MATERIALS AND METHODS

2.1. Dimensional analysis

Using the Buckingham Π method, effective parameters have been dimensionally analyzed. The scouring depth and length are considered a function of the following variables (Equation (1)).

$$D_{\max}, L_{\mathrm{S}} = f_1(q, d, B, d_{\mathrm{s}}, y_{\mathrm{A}}, y_{\mathrm{D}}, y_{\mathrm{E}}, x, x_{\mathrm{g}}, n, t_{\mathrm{s}}, g, \rho, \rho_{\mathrm{s}}, \mu) \tag{1}$$

where D_{max} is the maximum scouring depth, L_S is the maximum length of scour hole, q is the flow rate per unit width, d is the gate opening value, B is the channel width, y_A is the *vena contract* flow depth, y_D is the initial depth after the screen, y_E is the secondary depth after the screen, x is the distance between the screen and the sluice gate, x_g is the distance of the gate from the beginning of the channel, n is the porosity of screen, t_S is the thickness of the screens, ρ_S is the density of sediment particles, ρ is water density, d_S is the sediment particle size, g is gravity, and μ is dynamic viscosity. By using the Buckingham

Π method and considering repeated variables g, ρ, and d_S, the dimensionless expression is found to be:

$$\frac{d_S}{D_{max}}, \frac{d_S}{L_S} = f_3\left(\mathrm{Fr}_D, \frac{d}{d_S}, \frac{B}{d_S}, \frac{y_A}{d_S}, \frac{y_D}{d_S}, \frac{y_E}{d_S}, \frac{x}{d_S}, \frac{x_g}{d_S}, \frac{\rho_S}{\rho}, \frac{t_S}{d_S}, n, \frac{\mu}{\rho d_S^{1.5} g^{0.5}} = \mathrm{Re}_*\right) \quad (2)$$

Assuming that the values of t_S, n, x_g, x, B, d, and ρ_S are constant and the insignificant effect of parameters y_A, y_E, and Re_* on the maximum depth and length of scouring, the above equations are summarized as Equation (3).

$$\frac{d_S}{D_{max}}, \frac{d_S}{L_S} = f_3\left(\mathrm{Fr}_D, \frac{y_D}{d_S}, \frac{t}{t_a}\right) \quad (3)$$

The effect of adding clay and the combination of clay and montmorillonite nanoclay to the sedimentary material downstream of the screens has been investigated in order to reduce the scour profile. The experimental conditions of Table 1 were used. It was determined with the preliminary tests that the sand with an average diameter of 1.8 mm and a standard deviation of 1.28 mm is suitable for use.

2.2. Experimental equipment

To perform the experiments, a channel with a rectangular cross-section with a length, width, and height of 5, 0.3, and 0.45 m, respectively, was constructed in the hydraulic laboratory of the University of Maragheh. In order to have a smooth surface with minimal roughness, the channel floor and walls are made of plexiglass. The channel flow is provided by two pumps, each with a maximum flow rate of 7.5 L/s. These pumps are connected to a small reservoir at the channel entrance. The flow rate is measured with two taps connected to two rotameters installed at the pump outlet. To create the supercritical flow, a sluice gate was used installed 1 m from the entrance to the channel. The distance between the sluice gate and the screens was also 1.5 m and its opening was 1 cm. This was kept constant during the experiments. The length and thickness of the sedimentary bed were determined experimentally according to the flow characteristics after the screens. In addition, the scouring value was obtained from the initial test.

The initial test showed that the scour hole length increases to 1 m at high flow rates. Also, the hole depth advances to the floor level. Based on this, the length of the sedimentary bed was determined to be 1.3 m, taking into account the appropriate distance to develop the length of the scour hole. The bed thickness was 11.4 cm, accounting for the appropriate depth to reduce scouring due to the flow. To create a sedimentary bed with a specific thickness, two smooth polyethylene sheets were used. The length of the first floor is 2.5 m from the channel entrance to the screen (the stilling basin area) and the length of the second floor is 40 cm, which is installed at a distance of 1.3 m after the screen (Figure 1).

The present research is designed for high Froude numbers. For this reason, a vertical sluice gate with an opening of 1 cm has been used to create high Froude numbers. To create a sedimentary bed, river materials with the mentioned specifications have been used.

To use nanomaterials, firstly, nanomaterials are dispersed, and after several steps, they are injected into the sedimentary bed. The remarkable thing is that the dispersed nanomaterials have been injected without any change in the sediment bed by injecting clay and montmorillonite nanoclay at regular intervals, which result in minimizing scouring. On the other hand, in addition to dispersing nanomaterials, it should also be noted that the uniform distribution of nanoclay in the sediment bed was done without agglomeration. Because if the distribution of nanoclay is done with agglomeration, positive results will not be obtained from these materials in order to reduce scouring.

Table 1 | Experimental conditions

Type of tests	Range of flow depth (*vena contracta*), cm	Range of Fr no. (*vena contracta*)	*Q* (L/s)	Number of tests
Control test (only sedimentary materials)	$0.0 \le y \le 7.62$	$5.13 \le Fr \le 5.5$	3, 5, 6.25	18
Mixing clay into the sedimentary bed				
Combination of clay and montmorillonite nanoclay				

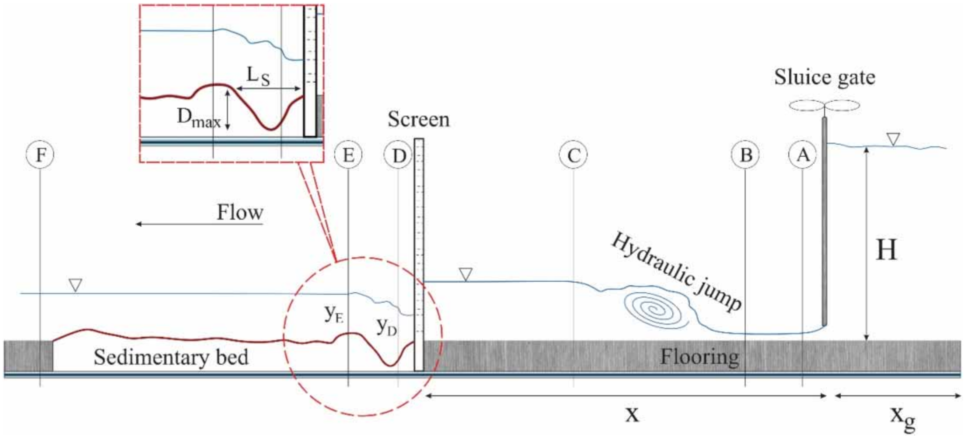

Figure 1 | An overview of the experimental equipment and the channel.

In Figure 1, section A is the starting point of the supercritical flow (*vena contracta*), section B is the starting point of the hydraulic jump, section C is the flow depth at the end of the hydraulic jump, section D is the beginning of the flow and the initial depth of the hydraulic jump after the screen, section E is the end of the hydraulic jump after the screen, and section F shows the downstream depth. The depth of the scour hole downstream of the screen has been measured at specific time intervals throughout the test. Due to the extreme changes in scouring depth with respect to time in the early stages of the experiment, the samples were measured at short intervals of 30 s (10 measurements), 5 min (4 measurements), 10 min (2 measurements), and finally for 30 min. In order to ensure the accuracy of the obtained results, the experiments have been repeated for the number of samples mentioned and for the three times as well. After collecting the data, we use the average of the calculated data as the final data. To determine the longitudinal and depth expansion of the scour hole downstream of the screen, at the end of each test, a point gauge and a digital camera were used and the entire bed profile was prepared using plot digitizer software. In this way, high-quality images of the flow passing through the screen and entering the mobile bed at specific times were recorded. At the end of each experiment, plot digitizer software was used to determine the longitudinal and depth expansion of the scour hole in the control section by taking a photo of the scour section with a camera. Also, in order to calibrate the points in the plot digitizer software, a very small computer millimeter label installed on the channel wall was used.

Figure 2 shows the graduated plates on the channel wall (a), the installed rotameters of the pumps to measure the flow rate (b), and the rod leveler (c) used in the current research.

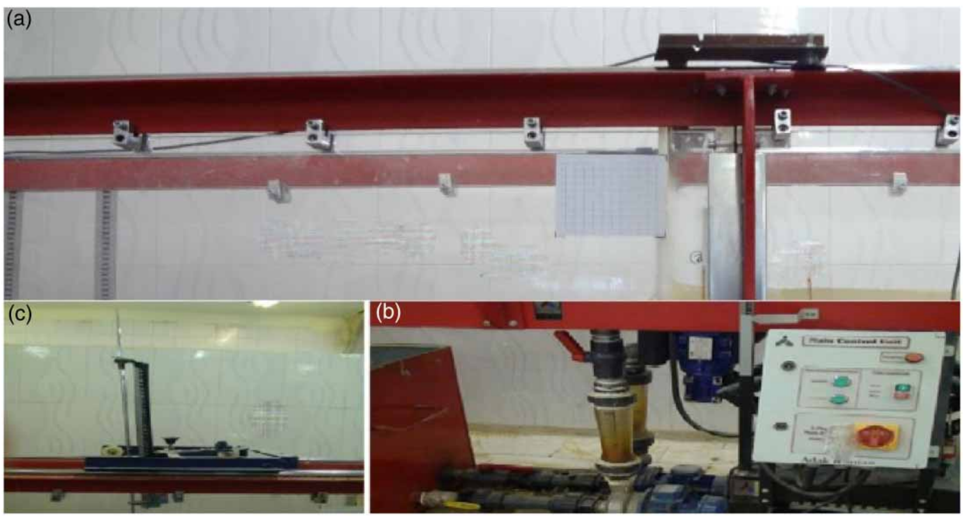

Figure 2 | Flow rate regulating rotameters and rod level gauges.

2.3. Characteristics of bed sediment particles

Equations presented by Yalin (1971) were used in order to determine the diameter of sediment particles. According to the research of Raudkivi & Ettema (1983), in order to prevent the formation of ripples in the alluvial bed of the channel and also to eliminate the cohesion of sediment particles, the average diameter of the particles should be larger than 0.7 mm. If the standard deviation of sediments obtained from the equation is less than 1.3, the material is uniform and if it is greater than 1.3, the material is nonuniform. Scouring depth in nonuniform sediments is lower than scouring depth in uniform sediments, and scouring depth decreases as the standard deviation of sediments increases (Melville 1997). In order to achieve uniform granulation in the sediments used in the experiments, the granulation of particles is usually expressed in the form of the weight percentage of the sample passed through standard sieves. In this study, sand with an average diameter of 1.8 mm and a standard deviation of 1.28 was selected. In this case, both maximum scouring is obtained and ripples are prevented. The granulation curve of bed sediments is presented in Figure 3 and the mechanical characteristics of bed sediments are presented in Table 2. For the second and third tests, about 90% of the sediment particles of the sand bed left from sieve #16 with the granularity specified in Figure 3, and the rest of the fine particles mixed with clay with the granularity specified in Figure 4 are presented.

It should be mentioned that since the calculated particle uniformity coefficient ($C_u = 1.61$) is less than 2, the materials can be considered as uniform particles (Lambe & Whithman 1969).

2.4. Characteristics of clay and nanoclay

The fine-grained soil in the coarse-grained bed, which makes up nearly 10% of its total, was classified based on the tests to determine the liquid limit (LL) and the plastic limit (PL) using the standard method ASTM D4318-87 and the hydrometric test of standard ASTM D421-58 based on Table 3. The fine-grain granulation curve is presented in Figure 4.

The nanoclay added to the channel bed is montmorillonite nanoclay. Montmorillonite nanoclays are a group of mineral clays whose structure consists of gibbsite surrounded by silica sheets on top and bottom and with van der Waals bonds. The length and width of these particles are in the range of a few tenths to 1.5 μm, and their third dimension is 1 nm with a significant difference in length and width (Uddin 2008). This product, after being added to fine-grained soils in a wet or dry method, improves the physical parameters of the soil by creating a chemical and physical reaction through cation and anion exchanges and by bonding and connecting nanoparticles and other soil particles. Research has shown that the addition of montmorillonite nanoclay up to 1% using the dry method and 0.5% using the wet method significantly improves shear

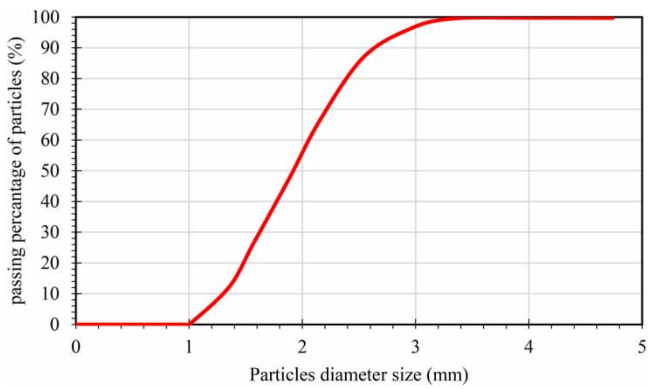

Figure 3 | Granulation curve of bed sediments (coarse grain).

Table 2 | Mechanical characteristics of bed sediments

	D10	D30	D60	σ_g	C_u	C_c
Sedimentary bed particles	1.3	1.7	2.1	1.28	1.61	0.69

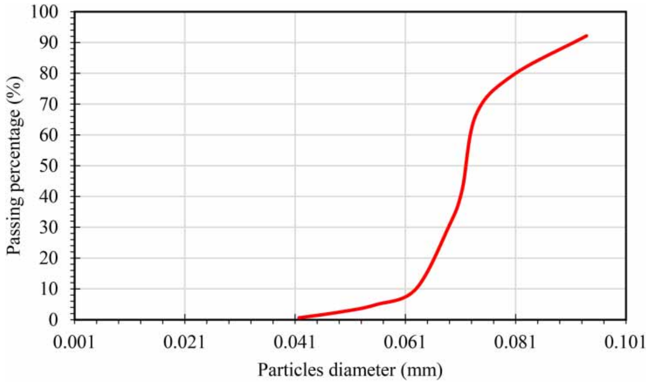

Figure 4 | Granulation curve of bed sediments (fine grain).

Table 3 | Clay specifications added to the bed

Group	Plasticity index (%)	PL (%)	LL (%)	Specific weight
CH	23.3	26.9	50.2	$G_S = 2.75$

resistance and reduces its permeability by 300–1,000 times (Zhang 2007). The physical and chemical characteristics of montmorillonite nanoclay are presented in Table 4.

The nanoclay used in this research was mixed with the required amount of water using a mixer with a high rotation speed and a suspension containing 1% of montmorillonite nanoclay that was uniformly added to the soil. The research shows that the major part of the increase in soil shear strength obtained from the equation is due to the increase in soil cohesion and the maximum value of the increase was observed at 1% (Mohammadi & Niazian 2013; Majeed *et al.* 2014). This phenomenon, as well as the decrease in permeability, reduces erosion. The shear strength of soil is a function of the friction angle and cementation between soil particles, and any improvement method, such as compaction or stabilization, focuses on the modification and improvement of one of those parameters. Unlike compaction methods that lead to an increase in ϕ, stabilization methods mainly emphasize improving cementation between soil particles. The assumption of uniform distribution of nanoclay in the sedimentary bed comes from the injection of nanoclay in networks with fixed and regular intervals.

Weakening of the effective parameters of friction angle and cohesion reduces the shear strength of the soil. Reducing soil permeability causes less contact of water with cement materials around soil particles. While preventing the deterioration of the shear resistance, it leads to the reduction of scour length and depth, compared to the permeable state.

3. RESULTS AND DISCUSSION

3.1. Experimental results

Figure 5 shows the development of the longitudinal profile of downstream scouring at three different flow rates without the addition of clay in the bed. In this figure, the vertical axis is the dimensionless ratio of scour depth to the channel width (Y/B) and the horizontal axis is the dimensionless ratio of scour length to the channel width (X/B). It can be seen that the increase in the flow rate passing through the screens has increased the depth and length of downstream scouring, so that by doubling the intensity of the flow, the depth and length of the scour have increased by 2.6 and 2.3 times, respectively. By comparing the

Table 4 | Clay specifications added to the bed

Mineral type	Particle size (nm)	Ion exchange coefficient (equivalent milliliters per 100 grams)	Special area (m^2/g)	Density (g/cm^3)	Color	Humidity (%)
Montmorillonite	1.18	48	250	0.6	Light yellow	1.5

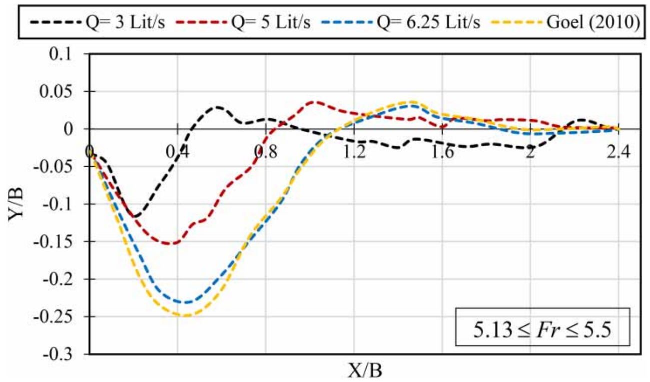

Figure 5 | Development of the longitudinal profile of scouring after the screen in three flow rates.

present research with Goel (2010) research for the sedimentary bed without adding clay and montmorillonite nanoclay, it shows the correctness of the results obtained. For comparison, a sediment bed without additives has been used at a flow rate of 6.25 L/s.

Figure 6 shows the changes in the relative downstream scouring depth with the addition of clay and nanoclay to the sedimentary materials at three different flow rates. In this figure, the vertical axis is the dimensionless ratio of scour depth to the maximum scour depth (d/D_{max}) obtained in the test and the horizontal axis is the dimensionless ratio of the desired time to the total test time (t/t_a). It can be seen that in the tested discharges, the maximum scour depth occurs at time $t/t_a = 1$. Also, with the addition of 10% of clay introduced for the second test and the addition of 1% of clay by weight as the percentage of montmorillonite nanoclay in the third test, the scouring depth decreased at all times. Also, the effect of clay and its combination with nanoclay has increased with the increase of the flow rate, so that in the most critical time of the test (30 min), the

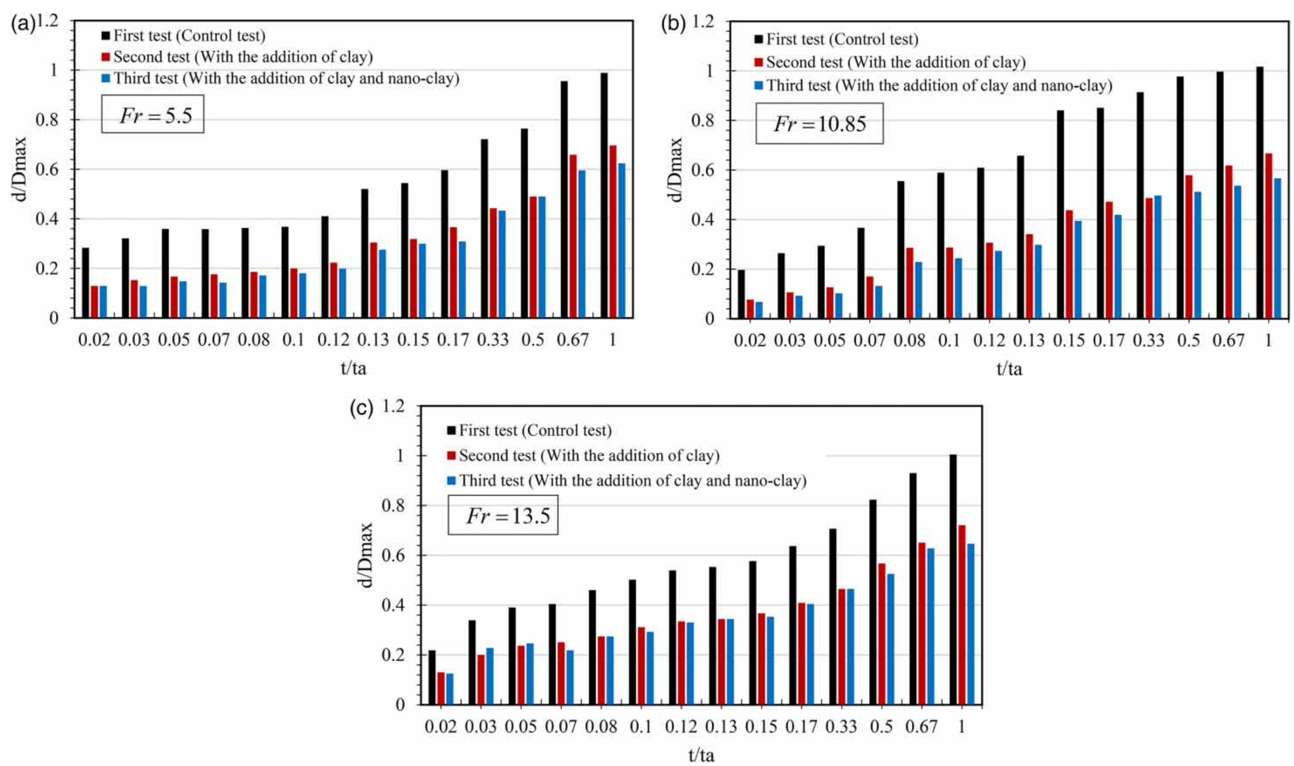

Figure 6 | Temporal changes of scouring depth with the addition of clay and its combination with montmorillonite nanoclay: (a) Fr = 5.5, (b) Fr = 10.58, and (c) Fr = 13.5.

greatest decrease in scouring depth occurred at a flow rate of 6.25 L/s. The reason for the increased shear strength of the substrate material is the use of montmorillonite nano-clay, which is clearly and completely mentioned in the text of the article. In this figure, the greater effect of nanoclay in increasing the cohesion strength of sedimentary particles and reducing its scouring rate due to mixing with clay and adding to sedimentary particles is evident, especially at high-flow rates.

Figure 7 shows the changes in the relative scouring length downstream of the screens, despite the addition of clay and nano-clay to the sediment materials at three different flow rates. In these graphs, the vertical axis is the dimensionless ratio of the scouring length to the maximum scouring length obtained (l/L_{max}), and the horizontal axis is the dimensionless ratio of the target time to the total test time (t/t_a). As with the scouring depth results, it can be seen that the addition of clay and its combination with nanoclay has reduced the scouring length at all times. The positive effect of clay and its combination with montmorillonite nanoclay is also evident in reducing the expansion of scouring length, and as a result of its use, the scouring length has decreased by 33%.

Also, with the addition of clay and the combination of clay and nano montmorillonite, there is an average decrease of 39 and 46% in scouring depth, respectively. This improvement and the positive effect of clay and especially its combination with montmorillonite nanoclay on increasing the cohesion strength of sediment particles and increasing the shear strength of particles are more evident at high-flow rates.

For a further analysis of the above results, the time changes in the scouring depth reduction percentage due to the addition of clay and its combination with montmorillonite nanoclay for the three flow rates tested are presented in Figure 8. In the two graphs of Figure 8, it can be seen that the greatest reduction in scouring occurred at the maximum flow rate (6.25 L/s). Also, the positive effect of the combination of clay and montmorillonite nanoclay when compared to the addition of clay to sediment particles is evident in reducing scouring, especially in the maximum discharge, so that the greatest reduction is in the third discharge. In the third experiment, the amount of scouring depth in the first time of the experiment was recorded as 66.3 and 44.4% after 30 min of the flow entering the control section. The lowest impact of the reduction in scouring depth downstream of the screen at the minimum flow rate (3 L/s) and with the addition of clay to the sediment particles was close to 28.2%.

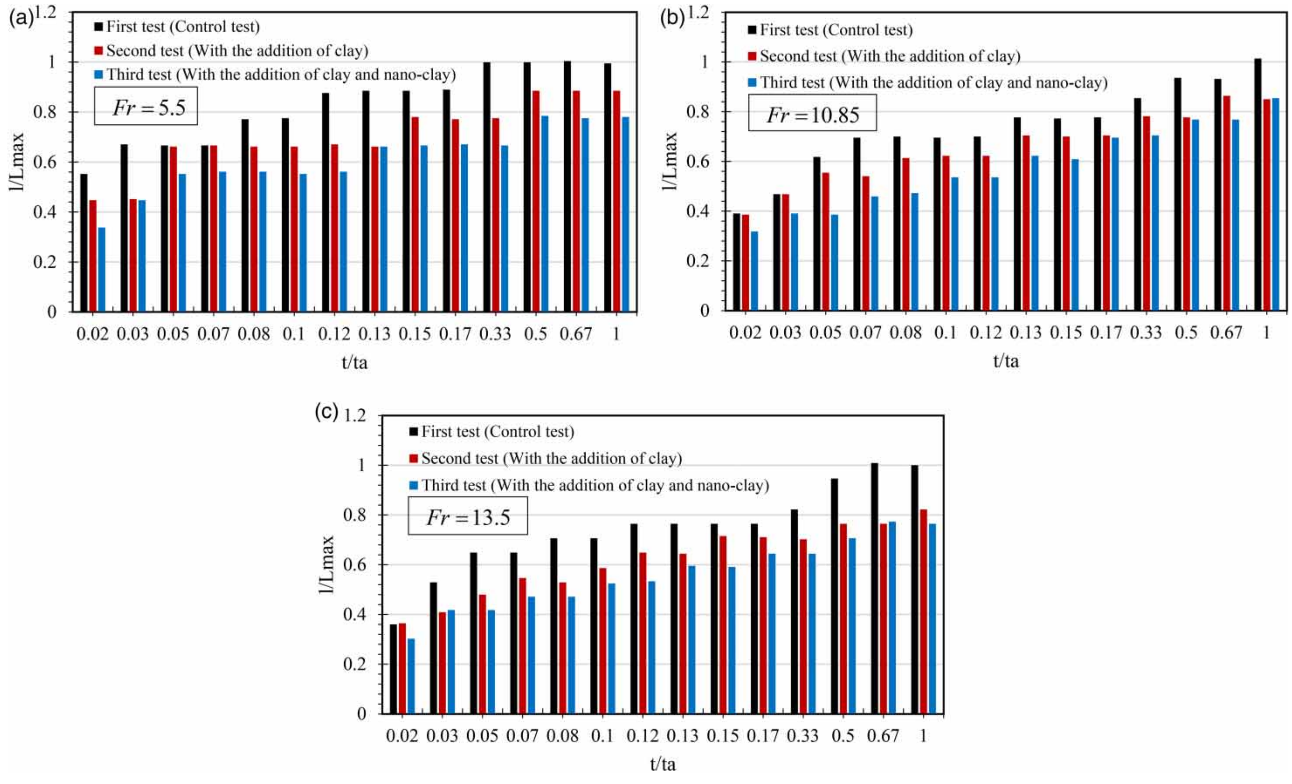

Figure 7 | Temporal changes of scouring length with the addition of clay and its combination with montmorillonite nanoclay: (a) Fr = 5.5, (b) Fr = 10.58, and (c) Fr = 13.5.

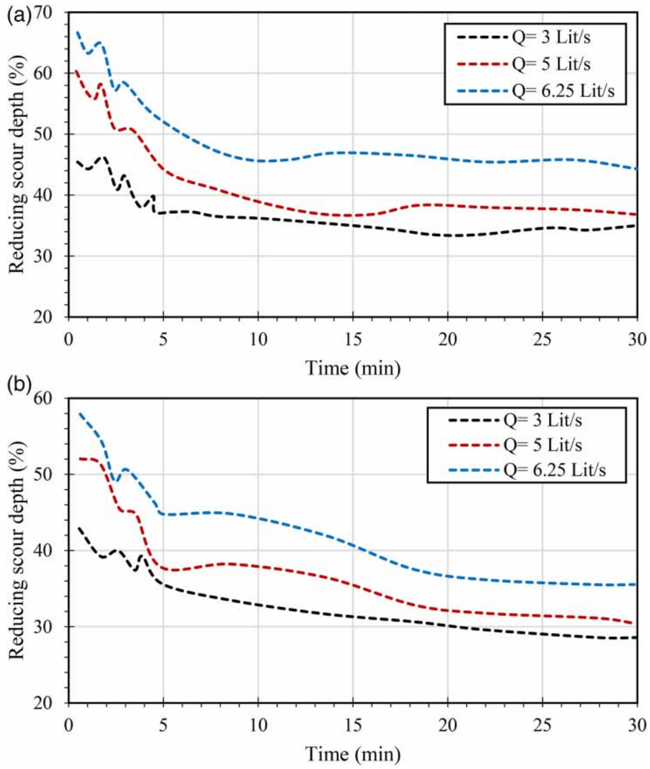

Figure 8 | Graph of changes in the time percentage of scouring depth reduction due to the addition of (a) clay to sedimentary particles and (b) a combination of clay and montmorillonite nanoclay to sedimentary particles.

In other words, it can be seen that the combination of clay and montmorillonite nanoclay can be used in flood discharges and downstream hydraulic structures, especially in areas where there is a high possibility of heavy rains and floods. In those places, it can be useful in further reducing erosion and scouring downstream structures.

Figure 9 shows the condition of the profile of scouring depth of the channel bed in the three mentioned tests for the maximum flow rate ($Q = 6.25$ L/s). It can be seen here that in the second and third tests, at the measurements (30 min), the scour depth has decreased from about 6.91 to about 4.5 and 3.52 cm, respectively. Also, the length of scour downstream of the screen has been limited from about 36 to 28 and 24 cm in the second and third experiments.

Figure 10 shows the longitudinal profile of scouring after-screen materials without using clay and montmorillonite nanoclay and with their addition at a flow rate of 6.25 L/s. In this figure, you can also clearly see the positive effect of clay and its combination with nanoclay in reducing the depth and length of the scouring profile.

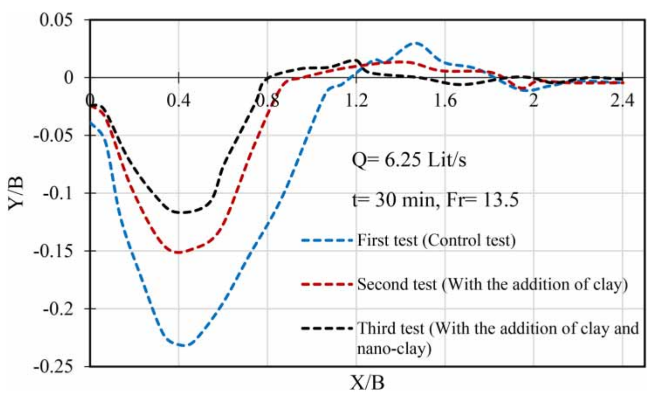

Figure 9 | Comparison of a longitudinal scouring profile in case of adding clay and combining it with nanoclay.

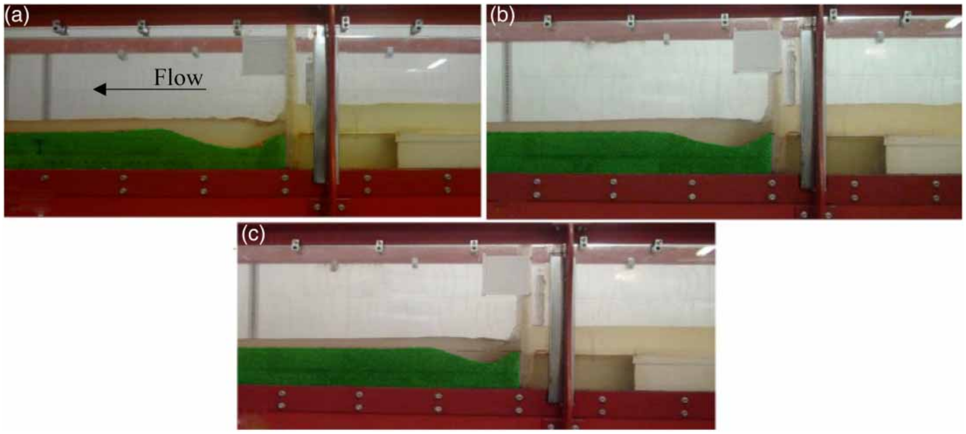

Figure 10 | A view of the longitudinal profile of scouring: (a) without using clay and montmorillonite nanoclay, (b) with the addition of clay, and (c) with the addition of clay and montmorillonite nanoclay combination.

The addition of nanoclay increases the shear strength of clay and sandy-clay soils. This increase in shear strength effectively prevents the increase of abrasion. On the other hand, by carefully looking at the results and especially Figures 5–9, it can be concluded that the use of nonstructural methods can be a very important and effective factor in the scouring of the bed, which includes the scouring depth and length. Some of these nonstructural methods compared to structural methods, in addition to reducing related costs, prevent damage to the environment and water resources. According to the materials used in this research, it can be concluded that due to the compatibility of montmorillonite nanoclay with the environment, in addition to the drastic reduction of the two parameters mentioned above, there is no environmental damage to the river, aquatic life, ecology of the river, and even the existing vegetation does not reach it. As mentioned above, using clay and the combination of montmorillonite clay and nanoclay, the scouring depth has decreased by 35 and 49%, respectively, compared to the case without additives. On the other hand, due to the high rate of leaching in nature, this material can be easily obtained from nature. These results have been obtained while the supercritical flow regime with high Froude numbers has occurred with a hydraulic jump on the sedimentary bed and high energy dissipation without disintegration of the sedimentary bed with the performance of nanomaterials. On the other hand, if we look at the issue from a geotechnical point of view, we will reach the conclusion that the existing bed gets its major shear strength from intergranular interlocking due to angular particles. Adding clay to the sedimentary bed creates proper cementation and increases the shear strength of the soil. In fact, adding clay improves the structure of cementation and increases the shear strength of clay and the substrate.

3.2. Statistical analysis results

In order to enrich the present research, statistical analysis has also been done on the data obtained from the experimental results. The Software Table Curve and SPSS were used for statistical analysis and the estimates made are mostly nonlinear. The Model Table Curve was used to obtain and evaluate the predicted data, the results of which are presented in Figures 11 and 12, and Model SPSS was used to calculate the Max, Min, and Ave. values, the results of which are presented in Table 5. According to Table 5, it can be concluded that the highest values of Max, Min, and Ave. are for the control test model (without clay and nanoclay) and on the other hand, the lowest value of the mentioned parameters is related to the combined model of clay and montmorillonite nanoclay. On the other hand, with the increase of the Froude number, the depth and length of the relative scour increase, but this increase is less compared to the control test model. In other words, the statistical analysis carried out is also a confirmation of the experimental results mentioned in the above sections. By examining the predicted data using the model Table Curve, the results of which are presented in Figures 11 and 12, it can be seen that according to the evaluation parameters R^2 and root mean square error (RMSE), a very favorable match between the experimental and predicted data has been achieved, the results of which are presented in Table 5.

4. CONCLUSION

In this research, the effect of adding clay and its combination with montmorillonite nanoclay to the building materials downstream of the energy-dissipating structure (screen) was investigated as a means to reduce the length and depth of scour.

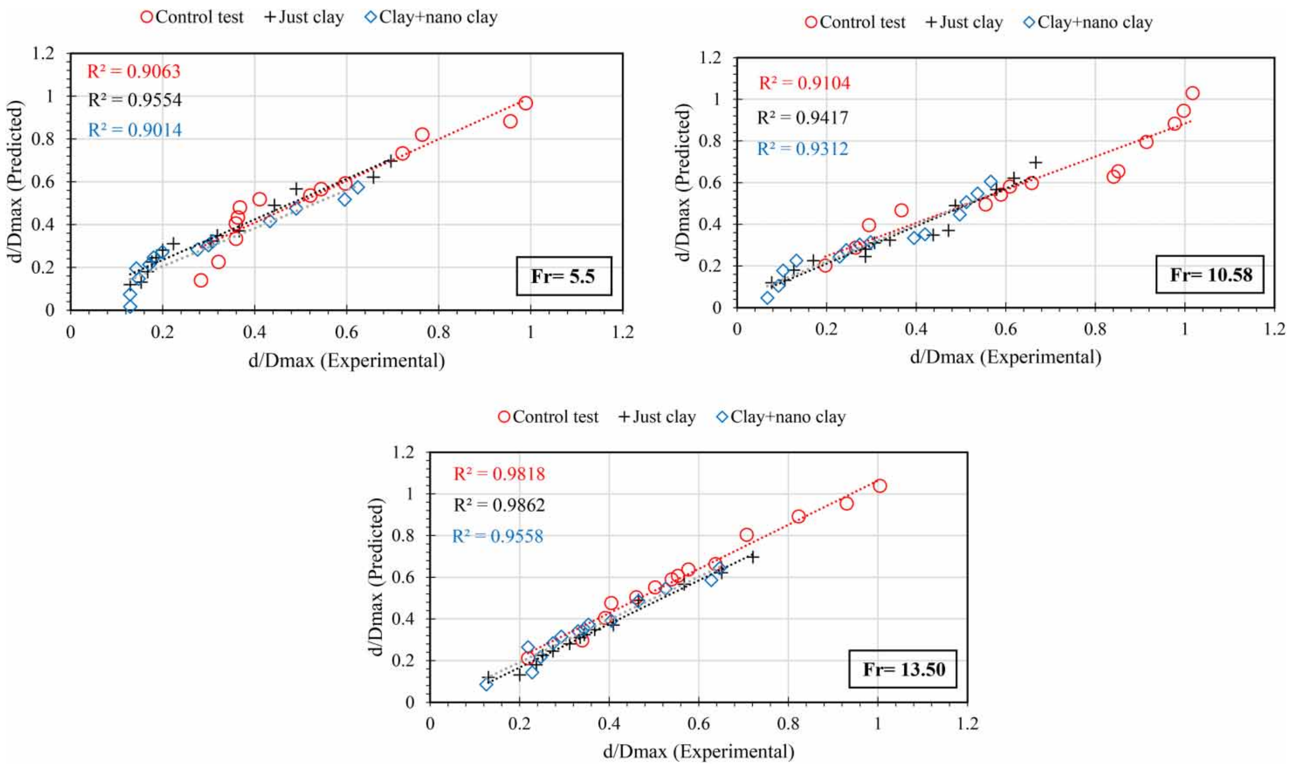

Figure 11 | Comparison of the experimental results of the relative scouring depth with the results of statistical analysis.

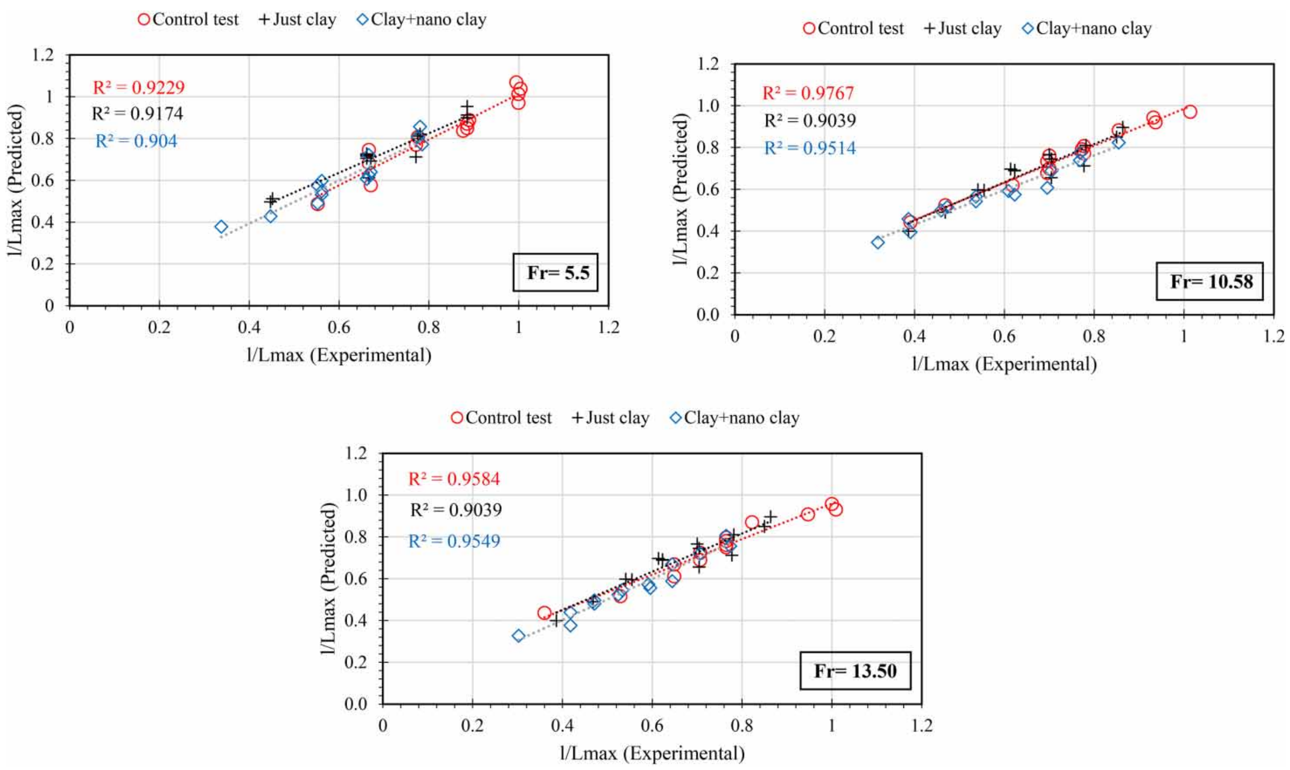

Figure 12 | Comparison of the experimental results of the relative scouring length with the results of statistical analysis.

Table 5 | Summary of statistical analysis results

Materials			Control test		Just clay		Clay + nanoclay	
Fr	t/t_a	Criteria	l/L_{max}	d/D_{max}	l/L_{max}	d/D_{max}	l/L_{max}	d/D_{max}
5.50	0.02–1.00	Min	0.552	0.283	0.447	0.129	0.338	0.129
		Max	1.004	0.989	0.885	0.696	0.785	0.624
		Ave.	0.831	0.540	0.705	0.322	0.613	0.295
		RMSE	0.047	0.071	0.049	0.047	0.042	0.053
		R^2	0.923	0.906	0.917	0.955	0.904	0.901
		Count	14					
10.58		Min	0.391	0.250	0.386	0.077	0.318	0.068
		Max	1.014	0.998	0.864	0.667	0.855	0.566
		Ave.	0.753	0.624	0.656	0.355	0.580	0.312
		RMSE	0.033	0.100	0.051	0.046	0.040	0.046
		R^2	0.977	0.910	0.904	0.941	0.951	0.931
		Count	14					
13.50		Min	0.360	0.219	0.364	0.130	0.302	0.126
		Max	1.009	1.005	0.822	0.721	0.773	0.647
		Ave.	0.745	0.625	0.621	0.376	0.561	0.363
		RMSE	0.039	0.051	0.061	0.033	0.028	0.033
		R^2	0.958	0.981	0.903	0.986	0.955	0.955
		Count	14					

The experimental results indicate the positive effect of clay and its combination with nanoclay on improving and reducing scouring depth and length, especially in the early section of data measurement downstream of the screen. Also, with the increase in discharge, the greatest reduction in scouring depth and length increases. In other words, at the maximum flow rate of 6.25 L/s and at the end of the measurement time (30 min), the maximum scouring depth was about 6.91 cm in the first test. With the addition of clay and the combination of clay with montmorillonite, nanoclay has decreased by about 35 and 49%, respectively. The positive effect of clay and its combination with montmorillonite nanoclay is also related to the reduction of scouring spread, so that the initial scouring length (36 cm) is decreased by 19.5 and 33%, respectively, for the claim and the combination of clay/montmorillonite nanoclay.

These results indicate the remarkable success of clay and nanoclay in controlling the scouring bed erosion downstream of hydraulic structures, especially in flood discharges. Considering that clay and nanoclay are compatible with the environment and are economical and accessible, it has a good compatibility with river systems and their ecologies, its use in the screen application system is recommended to researchers, operators, and designers. It is also expected that by increasing the concentration of nanoclay materials in the channel bed, it is possible to witness a better performance of these materials in reducing the maximum depth of scouring at the location of hydraulic structures, especially downstream of the screens and during floods.

Considering some laboratory limitations, including access to nanomaterials and other laboratory limitations, the following suggestions can be put forward as suggested topics in future research, including the practical effect of adding nanoclay amounts of less than 1% and different granulations of the sedimentary bed, the effect of the diameter of the grid dissipators, and also the changes in the gate opening rate.

DATA AVAILABILITY STATEMENT

All relevant data are included in the paper or its Supplementary Information.

CONFLICT OF INTEREST

The authors declare there is no conflict.

REFERENCES

Abdelhaleem, F. S. F. 2013 Effect of semi-circular baffle blocks on local scour downstream clear-overfall weirs. *Ain Shams Eng. J.* **4**, 675–684.
Bozkus, Z., Çakır, P. & Ger, M. 2007 Energy dissipation by vertically placed screens. *Can. J. Civ. Eng.* **34**, 557–564.

Chabert, J. & Engeldinger, P. 1956 Etude des affouillements autour des piles de points (Study of scour atbridge piers). Bureau Central d'Etudes les Equipment d'Outre-Mer. *Laboratoire National d'Hydraulique, France*.
Chiew, Y. M. 1992 Scour protection at bridge piers. *J. Hydraul. Eng.* **118**, 1260–1269.
Elnikhely, E. A. 2016 Minimizing scour downstream of spillways using curved vertical sill. In: *Proceedings of the 19th International Water Technology Conference*, Apr. 21–23, Sharm El Sheikh, Egypt.
Elsebaie, H. I. 2013 An experimental study of local scour around circular bridge pier in sand soil. *Int. J. Civ. Environ. Eng.* **13**, 23–28.
Goel, A. 2010 Scour investigations behind a vertical sluice gate without apron. *Pac. J. Sci. Technol.* **11**, 59–65.
Jia, Y. Y., Yao, Z. D., Duan, H. F., Wang, X. K. & Yan, X. F. 2022 Numerical assessment of canopy blocking effect on partly-obstructed channel flows: from perturbations to vortices. *Eng. Appl. Comput. Fluid Mech.* **16**, 1761–1780.
Karimaee, M. & Zarrati, A. R. 2011 Effect of collar on time development and extent of scour hole around cylindrical bridge piers. *Int. J. Eng.* **25**, 11–16.
Lambe, T. W. & Whithman, R. V. 1969 *Soil Mechanics. SI Version*. John-Wiley, New York.
Lee, S. O., Seungh, K. & Sturm, T. W. 1961 *Comparison of Laboratory and Field Measurements of Bridge Pier Scour*. U.S. Geological Survey, USA.
Li, P., Li, G., Guo, L. & Shi, D. 2021 A study on sediment avoidance diversion and the coordinated dispatch of water and sediment at an injection-water supply project on a sediment-laden river. *Eng. Appl. Comput. Fluid Mech.* **15**, 530–548.
Lu, S., Li, S., Liu, Z., Gao, X., Zhang, L. & Sun, C. 2021 Hydrochemical evolution of pore water in riverbed sedimentation zone during riverbank infiltration. *AQUA Water Infrastruct. Ecosyst. Soc.* **70**, 696–709.
Majeed, Z. H., Taha, M. R. & Jawad, I. T. 2014 Stabilization of soft soil using nanomaterials. *Res. J. Appl. Sci. Eng. Technol* **8**, 503–509.
Melville, B. W. 1997 Pier and abutment scour: integrated approach. *J. Hydraul. Eng.* **123**, 125–136.
Mohammadi, M. & Niazian, M. 2013 Investigation of nano-clay effect on geotechnical properties of Rasht clay. *Int. J. Adv. Sci. Tech. Res.* **3**, 37–46.
Nasr-Allah, H. T., Yasser, A. M., Mohamed, A. G. & Shawky, A. 2016 Experimental and numerical simulation of scour at bridge abutment provided with different arrangements of collars. *Alexandria Eng. J.* (in ress). doi:10.1016/j.aej.2016.01.021.
Qasim, R. M., Mohammed, A. A. & Abdulhussein, I. A. 2022 An investigating of the impact of bed flume discordance on the weir-gate hydraulic structure. *HighTechnol. Innovation J.* **3**, 341–355.
Rajaratnam, N. & Hurtig, K. I. 2000 Screen-type energy dissipator for hydraulic structures. *J. Hydraul. Eng.* **126**, 310–312.
Raudkivi, A. J. & Ettema, R. 1983 Clear-water scour at cylindrical piers. *J. Hydraul. Eng. ASCE* **109**, 338–350.
Sadeghfam, S., Akhtari, A. A., Daneshfaraz, R. & Tayfur, G. 2014 Experimental investigation of screens as energy dissipaters in submerged hydraulic jump. *Turk. J. Eng. Environ. Sci.* **38**, 126–138.
Sanoussi, A. A. & Habib, E. A. 2008 Local scour at rounded and sloped face with skew angles. In: *Proceedings of the International Conference on Construction and Building Tecnology*, June 16–20, Kuala Lumpur, Malaysia.
Singh, S. M. & Maiti, P. R. 2012 Local scour around a circular pier in open channel. *Int. J. Emerg. Technol. Adv. Eng.* **2**, 454–458.
Sun, X., Bi, Y., Karami, H., Naini, S., Band, S. S. & Mosavi, A. 2021 Hybrid model of support vector regression and fruit fly optimization algorithm for predicting ski-jump spillway scour geometry. *Eng. Appl. Comput. Fluid Mech.* **15**, 272–291.
Tuna, M. C. & Emiroglu, M. E. 2011 Scour profiles at downstream of cascades. *Sci. Iran.* **18**, 338–347.
Tuna, M. C. & Emiroglu, M. E. 2013 Effect of step geometry on local scour downstream of stepped chutes. *Arab. J. Sci. Eng.* **38**, 579–588.
Uddin, F. 2008 Clays, nano-clays, and montmorillonite minerals. *Metall. Mater. Trans. A* **39**, 2804–2814.
Widyastuti, I., Thaha, M. A., Lopa, R. T. & Hatta, M. P. 2022 Dam-break energy of porous structure for scour countermeasure at bridge abutment. *Civ. Eng. J.* **8**, 3939–3951.
Yalin, M. S. 1971 *Theory of Hydraulic Models*. Macmillan, London.
Zarrati, A. R., Gholami, H. & Mashahir, M. B. 2004 Application of collar to control scouring around rectangular bridge piers. *J. Hydraul. Res.* **42**, 97–103.
Zhang, G. 2007 Soil nanoparticles and their influence on engineering properties of soils. In *Geo-Denver Congress: New Peaks in Geotechnics*, Feb. 18–21, Denver, Colorado, USA.

First received 12 May 2023; accepted in revised form 11 June 2023. Available online 21 June 2023